High Photocatalytic Performance of Modified Bismuth Oxychloride Semiconductor under Sunlight

PREEJA. P. THATTIL and A. LEEMA ROSE*

Department of Chemistry, Holy Cross College (Autonomous), Affiliated to Bharathidasan University, Tiruchirappalli-620 002, Tamil Nadu, India.
*Corresponding author E-mail: leemarose25@gmail.com

ABSTRACT

In recent years, the bismuth compounds have gained much interest due to their potential applications in the field of Photocatalysis. In our present work, Bismuth oxychloride Photocatalyst and Aluminium fluoride doped Bismuth oxychloride photocatalyst were synthesized by simple chemical methods using bismuth nitrate pentahydrate as the precursor. The synthesized photocatalysts were characterized by different analytical techniques such as X-ray diffraction analyses, Ultraviolet-Diffuse reflectance spectrum, Field Emission-Scanning Electron Microscopy, Energy dispersive X-ray analyses, Fourier transform infrared spectroscopy studies and BET surface area analysis. The photocatalytic performances of the as-synthesized doped and undoped bismuth oxychloride photocatalyst were tested towards the degradation of Acid green 1 dye. The parameters such as the effect of pH, catalyst concentration and initial dye concentration are optimized, and the kinetic studies are carried out for the photocatalytic dye degradation process. The experimental results showed that about 80% of the Acid green 1 dye got decolourized within 90 min by effective air purging under natural sunlight radiation in the presence of the AlF-BiOCl photocatalyst under optimized conditions.

Keywords: AlF-BiOCl photocatalyst, XRD, HR-SEM, Acid green 1 dye, Air Oxidation, Solar radiation.

INTRODUCTION

Water pollution has become a major environmental concern as it encourages the transmission of many waterborne diseases, especially in developing nations. The paper, textile, leather, printing and dyeing industries which utilize a large amount of coloring materials such as dyes that are non-biodegradable and synthetically stable poisons are released into the nearby water bodies. This release of the effluent into the nearby water streams are considered to be a serious environmental hazard to both aquatic as well as human life[1]. Different water treatment techniques such as Coagulation, flocculation, adsorption, membrane separation, UV/Ozone treatment have been employed for the removal of the organic pollutants from the wastewater[2-5]. Among the various water treatment technologies, the development of advanced oxidation process in the past years have gained considerable interest by the researchers due to

the low-cost, eco-friendliness and the potential to completely degrade the organic pollutants into harmless products such as carbon dioxide and water[6-10]. Among many semi-conductor nanocatalysts bismuth-based semiconductors have gained tremendous consideration in the field of photocatalysis for its remarkable action against hazardous pollutants[11-13]. Bismuth oxychloride is reported to show excellent photocatalytic activity in the degradation of variety of organic pollutants such as dyes, pesticides, phenols and microbes as it possesses a high chemical stability[14]. Many researchers have reported the excellent photocatalytic activity of Bismuth oxychloride photocatalyst which is attributed to the layered structure of $[Bi_2O_2]^{2+}$ monolayer and dual 'Cl' layers[15]. However, its large band gap (3.17–3.54 eV) energy values have limited its activity as a photocatalyst towards many pollutants[16]. Hence, in order to overcome these limitations many modifications of bismuth oxychloride photocatalyst have been researched by the materials scientists in the recent years. Among which coupling and doping of the BiOCl photocatalyst with other suitable semiconductors are found to be effective in getting better photo-response and also facilitate the separation of photo induced electron–hole pairs which interact with the hydroxyl radicals to provide excellent photodegradation of the contaminants[17]. Hence, in our present work we have mainly focused on synthesizing a modified bismuth oxychloride photocatalyst via a facile low cost approach using water as the solvent, bismuth nitrate pentahydrate as the precursor, potassium chloride as the source of halogen and Aluminium fluoride as the dopant. The as-synthesized bismuth oxychloride photocatalyst have been employed for the degradation of the textile dye Acid green 1. It is a nitroso dye with the molecular formula ($C_{30}H_{15}FeN_3Na_3O_{15}S_3$) and Molecular Weight (878.46). The dye shows excellent absorption and excellent light fastness. It is mainly used in solar salt industry and wool, silk and nylon fabric dyeing and printing can also be used for leather dyeing[18,19]. The chemical structure and UV-Visible absorption spectrum of the Acid green 1 dye is shown in Figure 1.
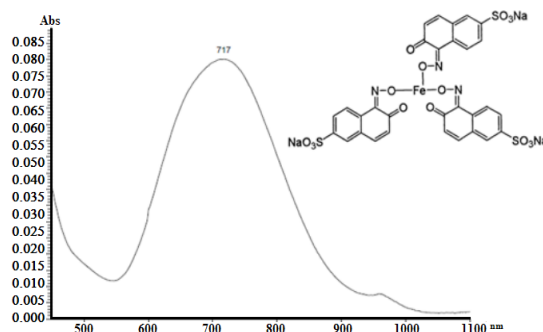

Fig.1. Shows the UV–Visible spectrum and Chemical structure of Acid green 1 dye

EXPERIMENTAL

Materials

All materials used in this experiment are of analytical grade. Bismuth nitrate pentahydrate (M.W. 485.07, purity 98%) and Acid green 1 dye was purchased from S. D. Fine Chemicals., Potassium chloride from Merck and ethanol (99.9%) was purchased from Changshu Hongsheng Fine Chemical Co. Ltd. The solution pH was measured using Elico digital pH meter. The decolourization of dyes was monitored by UV-Visible spectrophotometer (Hitachi-U2910).

Synthesis of AlF-BiOCl Photocatalyst

Bismuth nitrate pentahydrate is used as a precursor to prepare the bismuth oxychloride catalyst. In a typical synthesis, 0.1M bismuth nitrate pentahydrate is dissolved in 100 mL double distilled water. About 3 wt% of Aluminium fluoride salt is added to the precursor solution and it is continuously stirred for about half an hour and this solution is labeled as A. Potassium chloride is used as a source of chlorine which is dissolved in a minimum quantity of double distilled water labeled as solution B. The solution B is added to A and the mixture is stirred continuously for 30 minutes. The pH of the solution is adjusted to 2 using aqueous ammonia solution. The stirring is continued for 7 h and the obtained precipitate is repeatedly washed with double distilled water, dried in a hot air oven followed by calcinations process. 0.5, 1, 2 and 4 wt% of AlF/BiOCl photocatalyst is prepared by adopting the same procedure and bare Bismuth oxychloride catalyst is prepared without the addition of Aluminium fluoride as the dopant.

Characterization

The instrument UV-Spectrophotometer (Hitachi U2910) was used for measuring the decrease in absorbance of the dyes throughout the experiment for all the parameters optimized. The morphological characterizations of the synthesized AlF/BiOCl and BiOCl photocatalyst were investigated by HR-SEM with EDAX (FEI Quanta FEG 200-High Resolution Scanning Electron Microscope). The crystallinity and crystal phase of the as-synthesized photocatalysts were analyzed by X-ray diffraction (XRD, Rigaku) patterns with Cu-kα Radiation (λ = 1.54178 Å) in the range of 20–65 degree is scanned at 40 kV. The UV-DRS are carried out with the help of the instruments UV-Spectrophotometer SHIMADZU/UV-2600, BET surface area analysis using Quanta chrome instruments, Autosorb IQ series and Fourier transform infrared spectroscopy (Bruker Tensor-27) for the confirmation of the metal-oxide bond in the synthesized photomaterial.

Photocatalytic Degradation Experiments

About 1.13×10^{-5} mol/Lof Acid green 1 dye was prepared as the stock solution, from which required volume was withdrawn for each experiment. All the photocatalytic experiments were carried out on sunny days between 11 am to 2 pm. The suspensions were magnetically stirred in the dark for 15 min to attain adsorption-desorption equilibrium between dye and the catalyst. Before exposing the dye solution to sunlight irradiation, the initial absorption peak was recorded. To evaluate the effect of initial dye concentration, the concentration of the dye varied from 1.13×10^{-5} mol/L to 5.69×10^{-5} mol/L. The experiment was continued for 3 h at appropriate intervals small aliquots of the solution are withdrawn and the decrease in the absorbance is noted. The effect of pH was studied by adjusting the solution using NaOH and HCl. The blank experiments were performed in the dark at room temperature following the above procedure. The percentage decolourization was calculated using the formula

$$\frac{C0 - C}{C0} \times 100$$

Where C_0 is the concentration of the dye solution at t=0 and C is the concentration of the dye solution at time t.

RESULTS AND DISCUSSION

X-Ray Diffraction Analysis

The crystalline phase of the synthesized AlF-BiOCl and BiOCl photocatalyst is investigated by using powder X-ray diffraction analysis. The XRD pattern of the synthesized material is shown in Fig. 2a and 2b. The sharp diffraction patterns observed for the synthesized AlF doped BiOCl and bare BiOCl photocatalyst suggests that these photocatalysts are highly crystalline in nature. The diffraction peaks at 2θ positions 12.1, 24.2, 26, 32.5, 33.6, 36.7, 41, 46.7, 49.8, 55.2, 58.7, 68.2, 75.1, 77.6 corresponds to the crystal planes (001) (002) (101) (101) (102) (003) (112) (200) (004) (104) (212) (114) (220) (214) and (006) respectively, according to JCPDS card No. 85-0861. As no additional diffraction peaks are observed in the doped BiOCl photocatalyst or no other peaks are observed which might arise from impurity, it is concluded that the synthesized Bismuth oxychloride photocatalyst samples are pure. In the XRD pattern, the peak (102) is found with maximum intensity indicating it to be the preferred growth plane[20].
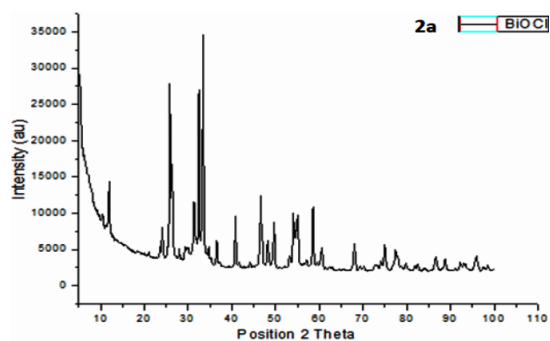

Fig. 2a. Shows the XRD pattern of the Synthesized Bismuth oxychloride photocatalyst
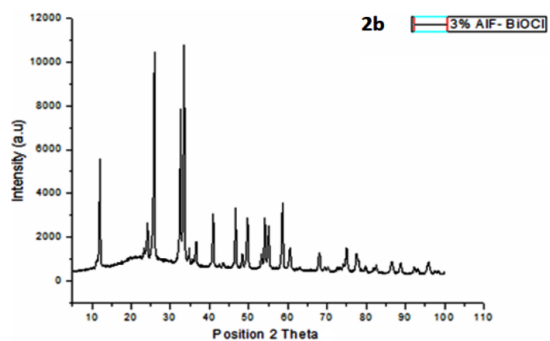

Fig. 2b. shows the XRD pattern of the synthesized AlF doped BiOCl photocatalyst

HR-SEM and EDAX Analysis

The morphology of the BiOCl and AlF doped BiOCl photocatalysts are studied from the scanning electron microscopic technique. It is found from the SEM micrographs that the synthesized Bismuth oxychloride photocatalyst possess nanoflake like structure and the width of the nanoflakes ranges from 69.3 to 75.1nm and the AlF-BiOCl photocatalyst also possessed flake-like arrangement which is shown in the SEM images Fig. 3a and 3b. Energy dispersive X-ray analysis is used to determine the major elemental composition in the synthesized materials[21]. Using this technique, the elemental composition of the synthesized materials is obtained with high resolution. The EDAX analysis data confirmed that the elements Bismuth, oxygen and chlorine are present in major composition without any other impurity in the BiOCl photocatalyst and the presence of aluminium, fluorine, Bismuth, oxygen and chlorine in the synthesized AlF-BiOCl photocatalyst is also confirmed from the EDAX data shown in Figure 4a and 4b.
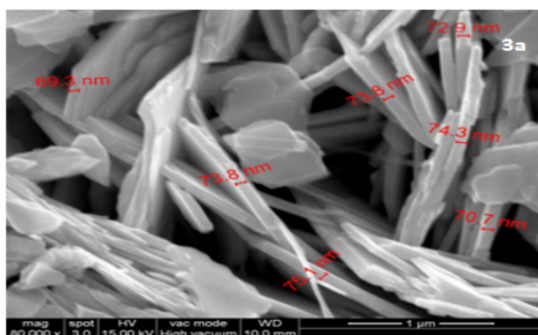

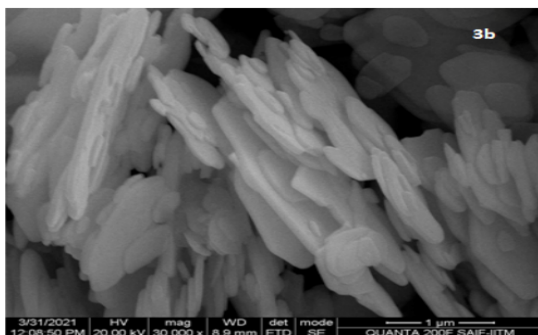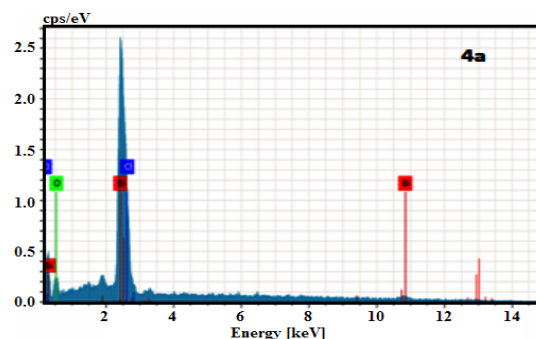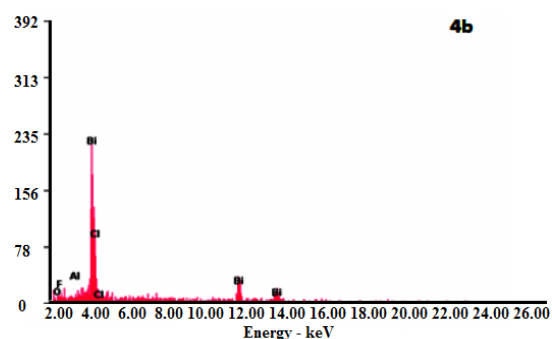**Fig. 4a. Shows the EDAX images of the synthesized Bismuth oxychloride photocatalyst**

Fig. 4b. Shows the EDAX images of the synthesized AlF-BiOCl photocatalyst

UV-Diffuse reflectance spectrum

The band gap measurements of the synthesized bismuth oxychloride and aluminium fluoride doped bismuth oxychloride photocatalyst is done with the help of UV-Visible diffuse reflectance spectroscopy which paves way to understand whether there are changes in the band gap of the modified semiconducting photomaterial and whether the photomaterial absorbs the UV or Visible radiation[22]. The band gap of the synthesized AlF-BiOCl and bare BiOCl photocatalyst is calculated using the following relation: $E_g = 1240/\lambda$, where λ is the cut off wavelength and E_g is the band gap energy in electron volts (eV). The band gap energy of the bismuth oxychloride photocatalyst is found to be 3.2ev and the band gap value of the Aluminium fluoride doped bismuth oxychloride photocatalyst is calculated to be 2.86ev.

Fourier Transform Infra-Red spectroscopy

The metal-oxygen bond formation in the synthesized AlF-BiOCl and bare BiOCl photocatalyst is confirmed from the fourier transform infra-red spectroscopy shown in Fig. 6. The band observed at 3435 cm^{-1} in both AlF-BiOCl and bare BiOCl photocatalyst corresponds to the stretching vibrations of hydroxyl group. The peak at 1630 cm^{-1} confirms

Fig. 3a. shows the FE-SEM images of the synthesized Bismuth oxychloride photocatalyst

Fig. 3b. Shows the FE-SEM images of the synthesized AlF-BiOCl photocatalyst

the bending vibrations of the water molecules which are adsorbed on the surface of the photocatalyst. The broad bands between 412 and 850 cm^{-1} are due to the framework vibrations of Bi-O bonds. The peak at about 532 cm^{-1} resulted from the symmetrical stretching vibration of the Bi-O band is a typical peak of BiOCl photocatalyst which is observed in both AlF-BiOCl and bare BiOCl photocatalysts[23-25].
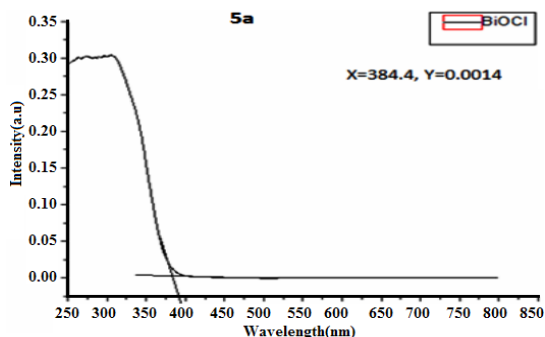

Fig. 5a. shows the UV-DRS plot of the synthesized Bismuth oxychloride photocatalysts
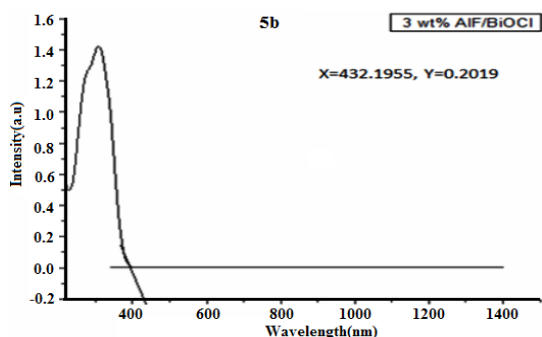

Fig. 5b. shows the UV-DRS plot of the synthesized Bismuth oxychloride and AlF-BiOCl photocatalysts
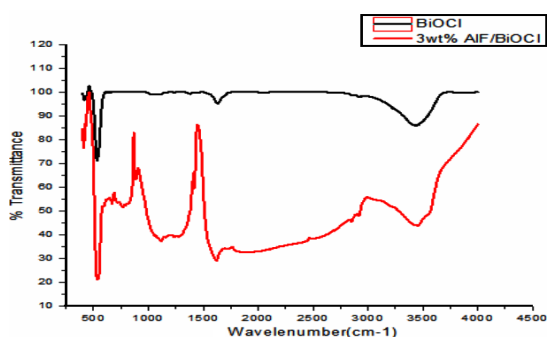

Fig. 6. Shows the FTIR spectrum of the synthesized BiOCl and AlF-BiOCl photocatalyst

BET Surface area measurements

Surface area is a crucial factor for determining the catalytic activity of the bare as well as surface modified photocatalysts[26,27]. The specific

surface area as well as the BJH pore size distribution of AlF-BiOCl and bare BiOCl photocatalysts are measured by Nitrogen adsorption-desorption isotherms and the plots are shown in Fig. 7a and 7b. The N_2 adsorption-desorption plots for samples BiOCl and AlF/BiOCl (3 wt%) are categorized as type IV isotherms, which proves the existence of pores in between each inter-crossed linked nanoplates[28,29]. From the BET surface area measurements, it is found that the specific surface area of the bismuth oxychloride photocatalyst is 18.726 m^2/g with a pore volume of 0.036 cc/g and the specific surface area of the AlF- Bismuth oxychloride photocatalyst is 14.837 m^2/g with a pore volume of 0.030 cc/g.
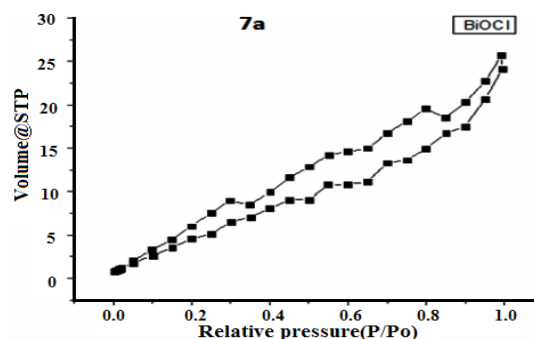

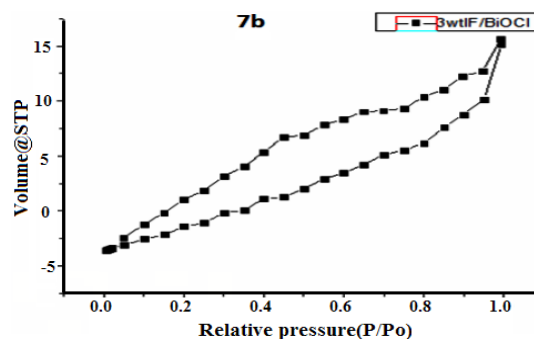Fig. 7a. Shows the Nitrogen adsorption–desorption isotherms of the synthesized BiOCl photocatalyst

Fig. 7b. shows the Nitrogen adsorption–desorption isotherms of the synthesized AlF-BiOCl photocatalyst

Photocatalytic Degradation studies of Acid green 1 dye
Effect of pH

The influence of pH on the photocatalytic decolourization of acid green 1 dye (1.13×10^{-5} mol/L) is studied by varying the pH range from 3 to 12 at a catalyst concentration of 15 mg per 50 mL of the dye solution. The maximum decolourization efficiency is observed at pH 5 which is shown in Fig. 8. The higher degradation of anionic acid green 1 dye at acidic pH = 5 is due to its interaction with the H$^+$ ions.

On the other hand, in alkaline medium the negatively charged BiOCl catalyst and the anionic acid green 1 dye competes for interaction with hydroxyl ions thereby resulting in low photocatalytic degradation process[30].
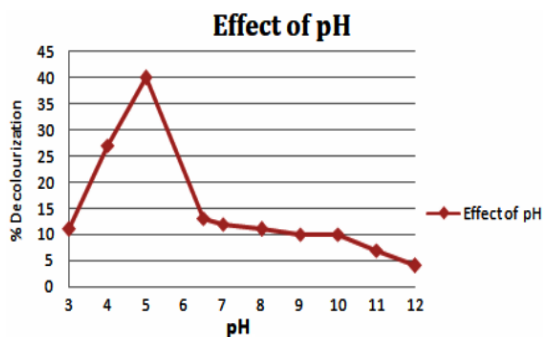

Fig. 8. 1.13×10^{-5} mol/L of acid green 1 dye solution, 25 mg of BiOCl catalyst, pH varied from 3 to 12, air flow rate = 2.5L/min under sunlight

Effect of Catalyst Concentration

For the effective decolourization of acid green 1 dye the bismuth oxychloride catalyst dosage is optimized by varying the catalyst concentration from 5 mg to 55 mg per 50 mL of the dye solution at optimized pH level 5. The maximum decolourization is observed for 15 mg of the catalyst dosage which is shown in Fig. 9. On increasing the BiOCl catalyst dosage a decrease in the photocatalytic dye decolourization process is observed. This may be due to the fact that on increasing the catalyst dosage the number of active surface area increases for the dye molecules to get adsorbed[31] and by adding excess amount of catalyst dosage, turbidity in the dye solution gets increased which in turn decreases the sunlight penetration as a result of which there is a decrease in the dye decolourization process.
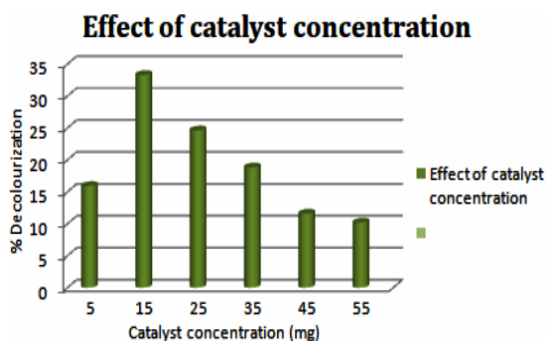

Fig. 9. 1.13×10^{-5} mol/L of acid green 1 dye solution, BiOCl catalyst dosage varied from 5 mg to 55 mg, pH = 5, air flow rate = 2.5L/min under sunlight

Effect of initial dye concentration

The initial dye concentration of the acid green 1 dye is varied in the range 1.13×10^{-5} mol/L to 5.69×10^{-5} mol/L to find out the maximum dye concentration that can be decolourized with bismuth oxychloride photocatalyst (15 mg/50mL of dye solution) at optimized pH level 5. The maximum decolourization of AG1 dye is observed at a concentration of 2.27×10^{-5} mol/L which is shown in Fig. 10. The experimental results shows that beyond the concentration level of 2.27×10^{-5} mol/L there is a decrease in the dye decolourization process, this may be due to the fact that at higher dye concentration levels the number of active sites of the bismuth oxychloride photocatalyst available for the dye molecules is very less and hence the probability of the dye molecule to react with the hydroxyl ions is less which shows a retardation in the dye decolourization process[32].
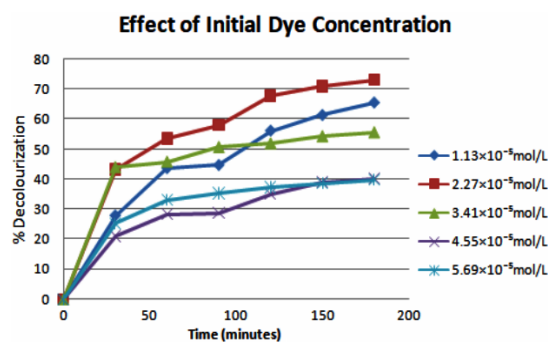

Fig. 10. 15mg of BiOCl catalyst, pH = 5, initial acid green 1 dye concentration varied from 1.13×10^{-5} mol/L to 5.69×10^{-5} mol/L, air flow rate = 2.5L/min under sunlight

Effect of Different weight percent of AlF onto BiOCl photocatalyst

The photocatalytic response of both doped and undoped bismuth oxychloride photocatalyst is studied by doping different weight percent (0.5, 1, 2, 3 and 4 wt%) of aluminium fluoride which is shown in Fig. 11. The maximum dye decolourization is observed for 3 wt% of aluminium fluoride doped bismuth oxychloride photocatalyst within 90 min whereas the bare BiOCl photocatalyst degraded AG1 dye only at 180 min under similar experimental conditions and under dark condition in the absence of the sunlight only 18% of the dye got decolourized this may be due to the adsorption of the AG1 dye onto the photocatalyst surface. The faster degradation of AG1 dye with AlF-BiOCl photocatalyst may be attributed to the decrease in size of the catalyst with the surface area. Greater

the surface-active sites available, greater will be the photocatalytic activity. A second factor responsible for the increase in photocatalytic degradation is the decrease in the band gap energy values. Generally, in a semiconductor the decrease in the band gap values causes generation of electrons and holes more quickly which further reacts with the hydroxyl radicals to degrade the dye molecules[33].
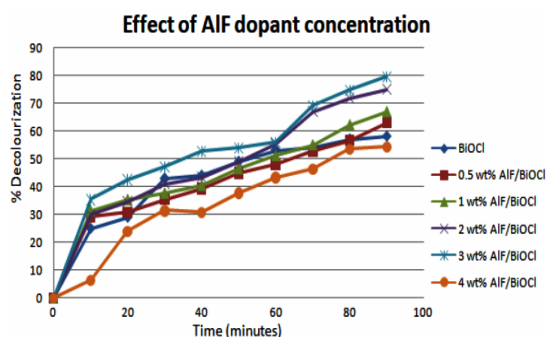

Fig. 11. shows the variation for different weight percent of AlF dopant concentration onto BiOCl catalyst for the photocatalytic decolourization of Acid green 1 dye

Kinetic studies

Langmuir-Hinshelwood (L-H) kinetic model is used here to study the kinetics of doped and undoped heterogeneous semiconductor photocatalyst. This (L-H) kinetic model has been widely used by several authors to find out the order of the reaction in heterogeneous semiconductor photocatalysis[34-37]. The kinetic studies carried out for the photocatalytic degradation of AG1 dye follows pseudo first order kinetics according to the equation.

$$\ln [C_0]/[C] = kt$$

Where k is the pseudo-first-order rate constant (min⁻¹), C_0 is the concentration of dyes (g L⁻¹) at t = 0, C is the concentration of dyes at reaction time t (minute). The linear fit between $\ln [C_0/C]$ and irradiation time 't' for bismuth oxychloride and Aluminium fluoride (0.5, 1, 2 and 3 wt%) doped bismuth oxychloride photocatalyst is shown in Fig. 12. The calculated average R^2 value for the bare bismuth oxychloride photocatalyst is 0.9514 and for different weight percent of AlF-BiOCl were found to be 0.9196, 0.9629 and 0.9095 respectively.
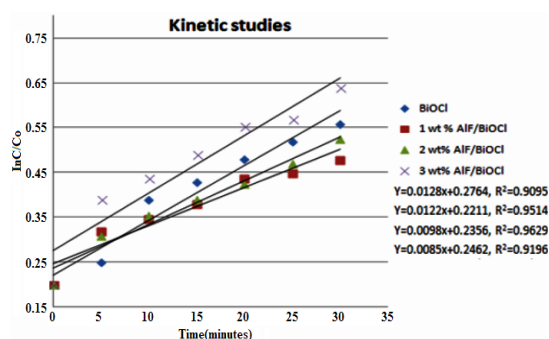

Fig.12. shows the pseudo-first order kinetic plot for the photocatalytic decolourization of Acid green 1 dye using different weight percent (0-3%) of Aluminium fluoride doped Bismuth oxychloride catalyst

CONCLUSION

Aluminium fluoride doped bismuth oxychloride and bare bismuth oxychloride photocatalyst is prepared via simple chemical precipitation technique. The optical and morphological characteristics of the synthesized BiOCl and AlF-BiOCl are studied and compared with the help of spectroscopy techniques such as XRD, FE-SEM, EDAX, FTIR, UV-DRS and BET surface area studies. The crystalline nature and hexagonal wurtzite structure of the synthesized BiOCl and AlF-BiOCl photomaterial is confirmed from the X-ray diffraction studies. The SEM images showed that the synthesized photomaterial possessed a flake-like structure and the major elements such as bismuth, oxygen, aluminium and fluorine in the synthesized photomaterial is confirmed from the EDAX data. The FTIR studies confirmed the metal-oxide bond formation and a decrease in the band gap and surface area of the AlF-BiOCl catalyst compared to that of the bare BiOCl photocatalyst is studied from the UV-DRS and BET surface area analysis. Further the photocatalytic activity carried out for the acid green 1 dye showed that AlF doped bismuth oxychloride photocatalyst degraded the dye within 90 min under sunlight radiation at optimized conditions whereas the bare bismuth oxychloride photocatalyst took more under similar optimized conditions. The photocatalytic reaction followed pseudo-first order kinetics according to Langmuir-Hinshelwood kinetic model. Thus, on concluding, AlF-BiOCl photocatalyst coupled with air oxidation under sunlight has proved to be an efficient photocatalyst for the degradation of the acid green 1 dye in aqueous solution.

Conflict of Interest

The authors declare that there is no conflict of interest.

REFERENCES

1. Brit., Synthetic Dyes: A look at Environmental & Human Risks., **2008**.
2. Matilainen, A.; Vepsäläinen, M.; Sillanpää, M., Natural Organic Matter Removal by Coagulation during Drinking Water Treatment: A Review. *Advances in Colloid and Interface Science*., **2010**, *159*(2), 189-97.
3. Liu, Y.; Zeng, G.; Tang, T., Highly effective adsorption of cationic and anionic dyes on magnetic Fe/Ni nanoparticles doped bimodal mesoporous carbon, *Journal of Colloid and Interface Science*., **2015**, *448*, 451–549.
4. Khulbe, K.C.; Matsuura, T., Removal of heavy metals and pollutants by membrane adsorption techniques, *Applied Water Science*., **2018**, *8*,19.
5. Laisheng, Li.; Zhu, W.; Zhang, P.; Lu, P., UV/O3-BAC process for removing organic pollutants in secondary effluents, *Desalination*., **2017**, *1-3*, 114-124.
6. Song, L.; Pang, Y.; Zheng, Y.; Ge, L., Hydrothermal synthesis of novel g-C3N4/BiOCl heterostructure nanodiscs for efficient visible light photodegradation of Rhodamine B, Appl. Phys. A: *Mater. Sci. Process*., **2017**, *123*, 500.
7. Pu, X.; Zhang, D.; Gao, Y.; Shao, X.; Ding, G.; Li, S.; Zhao, S., One-pot microwave-assisted combustion synthesis of grapheme oxide–TiO$_2$ hybrids for photodegradation of methyl orange, *J. Alloys Compd*., **2013**, *551*, 382–388.
8. Gao, X.; Zhang, X.; Wang, Y.; Peng, S.; Yue, B.; Fan, C., Rapid synthesis of hierarchical BiOCl microspheres for efficient photocatalytic degradation of carbamazepine under simulated solar irradiation, *Chem. Eng. J*., **2015**, *263*, 419–426.
9. Zhang, Y.; Zhang, Q.; Shi, Q.; Cai, Z.; Yang, Z., Acid-treated g-C3N4 with improved photocatalytic performance in the reduction of aqueous Cr (VI) under visible-light, *Sep. Purif. Technol*., **2015**, *142*, 251–257.
10. Yan, S.C.; Li, Z.S.; Zou, Z.G., Photodegradation of rhodamine B and methyl orange over boron-doped g-C3N4 under visible light irradiation, *Langmuir*., **2010**, *26*, 3894–3901.
11. Seddigi, Z.S.; Gondal, M.A.; Baig, U.; Ahmed, S.A.; Abdulaziz, M.A.; Danish, E.Y., Facile synthesis of light harvesting semiconductor bismuth oxychloride nano photo-catalysts for efficient removal of hazardous organic pollutants, *PLOS ONE*., **2017**, *12*(2),e0172218.
12. Shen, K.; Gondal, M.A.; Al-Saadi, A.A.; Liye, L.; Chang, X.; Xu, Q., Visible light induced photodegaradtion of Rhodamine dyes over BiOCl and the vital importance of frontier orbital energy of the dye molecules in the reaction kinetics, *Res. Chem. Intermed*., **2015**, *41*, 2753-2766.
13. Kang, S.; Pawar, R.C.; Pyo, Y.; Khare, V.; Lee, C.S., Size-controlled BiOCl±RGO composites having enhanced photodegradative properties, *J. Exp. Nanosci*., **2016**, *11*, 259-275.
14. Li, K.; Liang, Y.; Yang, J.; Gao, Q.; Zhu, Y.; Liu, S.; Xu, R.; Wu, X., Controllable synthesis of 001 facet dependent four square BiOCl nanosheets: a high efficiency photocatalyst for degradation of methyl orange, *J. Alloys. Compd*., **2017**, *695*, 238–249.
15. Wen.; Ren, W. L.; Peng, F., Recent advances of bismuth oxychloride photocatalytic material: Property, preparation and performance enhancement, *Journal of Electronic Science and Technology*, **2020**, *18*(2), 100020.
16. Liu, X.; Su, Y.; Zhao, Q.; Du, C.; Liu, Z., Constructing Bi$_{24}$O$_{31}$Cl$_{10}$/ BiOCl heterojunction via a simple thermal annealing route for achieving enhanced photocatalytic activity and selectivity, *Sci. Rep. Sci*., **2016**.
17. Zhao, H.; Tian, F.; Wang, F.; Chen, R., A Review on Bismuth-Related Nanomaterials for Photocatalysis, *Reviews in Advanced Sciences and Engineering*., **2014**, *3*, 1–25.
18. Raue.; Roderich.; Corbett.; John F., Nitro and Nitroso Dyes, Ullmann's Encyclopedia of Industrial Chemistry., **2000**.

19. Horobin, R.W.; Kiernan, J.A., Conn's Biological Stains: A Handbook of Dyes, Stains and Fluorochromes for Use in Biology and Medicine, *BIOS Scientific. Publ.*, **2002**, *101*, 102.

20. Sharma, I.D.; Tripathi, G.K.; Sharma, V.K.; Tripathi, S.N.; Kurchania, R.; Kant, C.; Sharma, A.K.; Saini, K.K., One-pot synthesis of three bismuth oxyhalides (BiOCl, BiOBr, BiOI) and their photocatalytic properties in three different exposure conditions, *Cogent Chemistry.*, **2015**, *1*, 1076371.

21. Ascencio Aguirre, F.M.; Bazan Diaz, L.; Mendoza Cruz, R.; Vazquez, M.S.; Encinia, O.O.; Rodriguez, A.G.; Becerra, R.H., Chemical synthesis and characterization of bismuth oxychloride BiOCl nanoparticles, *Appl. Phys. A.*, **2017**, *123*, 155.

22. Sharma, K.; Dutta, V.; Sharma, S.; Raizada, P.; Hosseini Bandegharaei A.; Thakur, P.; Singh, P., Recent advances in enhanced photocatalytic activity of bismuth oxyhalides for efficient photocatalysis of organic pollutants in water: A review, *Journal of Industrial and Engineering Chemistry.*, **2019**.

23. Xie, T.; Xu, L.; Liu, C.; Yang, J.; Wang, M., Magnetic composite BiOCl-SrFe$_{12}$O$_{19}$: a novel p-n type heterojunction with enhanced photocatalytic activity, *Dalton Trans.*, **2014**, *43*, 2211–2220.

24. Fruth, V.; Popa, M.; Berger, D.; Ionica, C.M.; Jitianu, M., Phase investigation in the antimony doped Bi$_2$O$_3$ system, *J. Eur. Ceram. Soc.*, **2004**, *24*, 1295–1299.

25. Song, J.; Mao, C.; Niu, H.; Shen, Y.; Zhang, S., Hierarchical structured bismuth oxychlorides: self-assembly from nanoplates to nanoflowers via a solvothermal route and their photocatalytic properties, *Cryst. Eng. Comm.*, **2010**, *12*, 3875–3881.

26. Tian, F.; Xiong, J.; Zhao, H.; Liu, Y.; Xiao, S.; Chen, R., Mannitol-assisted solvothermal synthesis of BiOCl hierarchical nanostructures and their mixed organic dye adsorption capacities, *Cryst. Eng. Comm.*, **2014**, *16*, 4298–4305.

27. Wang, X.; Bi, W.; Zhai, P.; Wang, X.; Li, H.; Mailhot, G.; Dong, W., Adsorption and photocatalytic degradation of pharmaceuticals by BiOClxIy Nanospheres in aqueous solution, *Appl .Surf. Sci.*, **2016**, *360*, 240–251.

28. Di, J.; Xia, J.; Ji, M.; Wang, B.; Yin, S.; Zhang, Q.; Chen, Z.; Li, H., Carbon quantum dots modified BiOCl ultrathin nanosheets with enhanced molecular oxygen activation ability for broad spectrum photocatalytic properties and mechanism insight, *ACS Appl. Mater. Interfaces.*, **2015**, *7*, 20111–20123.

29. Qiao, R.; Mao, M.; Hu, E.; Zhong, Y.; Ning, J.; Hu, Y., Facile formation of mesoporous BiVO4/Ag/AgCl heterostructured microspheres with enhanced visible-light photoactivity, *Inorg. Chem.*, **2015**, *54*, 9033–9039.

30. Rashid, J.; Karim, S.; Kumar, R.; Barakat, M.A.; Akram, B.; Hussain, N.; Bin H.B.; Xu, M., A facile synthesis of bismuth oxychloride graphene oxide composite for visible light photocatalysis of aqueous diclofenac sodium, *Scientific Reports.*, **2020**, *10*, 14191.

31. Grilla, E.; Kagialari, M.N.; Petala, A.; Frontistis, Z.; Mantzavinos, D.; Photocatalytic Degradation of Valsartan by MoS$_2$/BiOCl Heterojunctions, *Catalysts.*, **2021**, *11*, 650.

32. Seddigil, Z.S.; Gondal, M.A.; Baig, U.; Ahmed, S.A.; Abdulaziz1, M.A., Danish, E.Y.; Khaled, M.M.; Lais, A., Facile synthesis of light harvesting semiconductor bismuth oxychloride nano photo-catalysts for efficient removal of hazardous organic pollutants, *PLOS ONE.*, **2017**.

33. Li, H.; Li, J.; Zhihui, Ai.; Jia, F.; Zhang, L., Oxygen Vacancy-Mediated Photocatalysis of BiOCl: Reactivity, Selectivity, and Perspectives, *Angew. Chem. Int. Ed.*, **2018**, *57*, 122-138.

34. Tanwar, R.; Mandal, U.K., Photocatalytic activity of Ni0.5Zn0.5Fe$_2$O$_4$@polyaniline decorated BiOCl for azo dye degradation under visible light-integrated role and degradation kinetics interpretation, *RSC Adv.*, **2019**, *9*, 8977.

35. Ramachandran, S.; Sivasamy, A., Synthesis of nanocrystalline bismuth oxide and its visible photocatalytic activity in the degradation of an organic dye, *Inorganic and Nano-Metal Chemistry.*, **2018**.

36. Cui, P.; Wang, J.; Wang, Z.; Chen, J.; Xing, X.; Wang, L.; Yu, R., Bismuth oxychloride hollow microspheres with highvisible-light photocatalytic activity, *Nano Research.*, **2015**.

37. Cao, B.; Dong, P.; Cao, S.; Wang, Y., BiOCl/Ag$_3$PO$_4$ Composites with Highly Enhanced Ultraviolet and Visible Light Photocatalytic Performances, *J. Am. Ceram. Soc.*, **2013**, *96*(2), 544–548.